NASA-TM-86437 19850022925

NASA Technical Memorandum 86437

USAAVSCOM Technical Memorandum 85-B-4

RESIDUAL THERMAL AND MOISTURE INFLUENCES ON THE STRAIN ENERGY RELEASE RATE ANALYSIS OF EDGE DELAMINATION

T. KEVIN O'BRIEN, I. S. RAJU AND D. P. GARBER

JUNE 1985

National Aeronautics and Space Administration

Langley Research Center
Hampton, Virginia 23665

Summary

A laminated plate theory analysis is developed to calculate the strain energy release rate associated with edge delamination growth in a composite laminate. The analysis includes the contribution of residual thermal and moisture stresses to the strain energy released. The strain energy release rate, G, increased when residual thermal effects were combined with applied mechanical strains, but then decreased when increasing moisture content was included. A quasi-three-dimensional finite element analysis indicated identical trends and demonstrated these same trends for the individual strain energy release rate components, G_I and G_{II}, associated with interlaminar tension and shear. An experimental study indicated that for T300/5208 graphite-epoxy composites, the inclusion of residual thermal and moisture stresses did not significantly alter the calculation of interlaminar fracture toughness from strain energy release rate analysis of edge delamination data taken at room temperature, ambient conditions.

Nomenclature

$[A]$	extensional stiffness matrix
A	delaminated area
a	delamination size
$[B]$	coupling stiffness matrix
b	half width of laminate cross section
$[D]$	bending stiffness matrix
E	modulus of elasticity
E_{LAM}	longitudinal laminate modulus
E^*	longitudinal modulus of laminate completely delaminated along one or more interfaces
E_{11}, E_{22}	lamina moduli parallel and perpendicular to fiber direction, respectively
F_{x1}, F_{x2}, F_{x3}	axial forces
G_{12}	lamina shear moduli
G	strain energy release rate
G_I, G_{II}, G_{III}	strain energy release rate components due to opening in-plane shear, and out-of-plane shear fracture modes
G^M, G^{M+T}, G^{M+T+H}	strain energy release rate due to mechanical, mechanical plus thermal, and mechanical plus thermal plus hygroscopic loading
G_c	critical strain energy release rate for delamination onset
G_{Ic}	critical mode I strain energy release rate for delamination onset
h	ply thickness
ℓ	length
N	number of plies
$\{N\}$	vector of force resultants
$\{M\}$	vector of moment resultants
$[\bar{Q}]$	transformed reduced stiffness matrix
t	laminate thickness

U	strain energy
u	strain energy density
u_{ek}	lamina strain energy density due to extension for the k^{th} ply
u_{bk}	lamina strain energy density due to bending for the k^{th} ply
u_{ck}	lamina strain energy density due to bending-extension coupling for the k^{th} ply
V	volume
w	width
x,y,z	laminate coordinate system
z_k	distance from laminate midplane to the bottom of the k^{th} ply
α_1	lamina coefficient of thermal expansion in the fiber direction
α_2	lamina coefficient of thermal expansion normal to the fiber direction
$\{\alpha\}_k$	lamina coefficients of thermal expansion in laminate coordinate system
$\{\bar{\alpha}\}$	laminate coefficients of thermal expansion
β_1	lamina coefficient of moisture expansion in the fiber direction
β_2	lamina coefficient of moisture expansion normal to the fiber direction
$\{\beta\}_k$	lamina coefficients of moisture expansion in the laminate coordinate system
$\{\bar{\beta}\}$	laminate coefficients of moisture expansion
ΔH	percentage moisture weight gain
ΔT	temperature differential from cure temperature to test temperature
ε	strain
ε_c	delamination onset strain
ε_{ij}	strain tensor
$\{\varepsilon\}$	vector of in-plane strain components
ε^o	mid-plane strain
$\varepsilon^M,\varepsilon^T,\varepsilon^H$	strain components due to mechanical, thermal, and hygroscopic loading

$\{\kappa\}$	vector of curvatures
$\{\bar{\lambda}\}$	laminate coefficients of thermal curvature
$\{\bar{\mu}\}$	laminate coefficients of moisture curvature
ν_{12}	Poisson's ratio in lamina coordinates
σ_{ij}	stress tensor
$\{\sigma\}$	vector of in-plane stress components

Introduction

Composite materials are currently being considered for primary structural applications that tax their ability to carry load after being damaged. In particular, the extensive delamination that may result from low-velocity impacts on a thick composite wing skin may severely limit the compressive strains the material can sustain, and hence, severely limit the weight saving potential of the composite [1,2]. Because of this limitation, there has been increased emphasis on developing and measuring improved delamination resistance in high performance composites [3,4]. One test recently proposed for measuring delamination resistance is the edge delamination tension (EDT) test which measures the mixed-mode interlaminar fracture toughness [5,6,7]. This EDT test involves measuring the strain at the onset of edge delamination during a tensile test of a composite laminate. The measured strain is then substituted into an equation for strain energy release rate to obtain the interlaminar fracture toughness. Although the mixed-mode nature of the edge delamination test has been examined [5,6,8,9], previous analyses have not considered the influence of residual thermal and moisture stresses on the strain energy release rate as edge delaminations grow. The purpose of this investigation was to modify existing analyses to account for the influence of residual thermal and moisture stresses on strain energy release rates for edge delamination, and to experimentally determine the significance of these thermal and moisture effects on interlaminar fracture toughness measurement.

Strain Energy Release Rate Analysis

Laminated Plate Theory

An equation was previously derived for the strain energy release rate, G, associated with edge delamination growth in a composite laminate [5]. This equation had the following form:

$$G = \frac{\varepsilon^2 t}{2} (E_{LAM} - E^*) \tag{1}$$

where ε = nominal tensile strain

t = laminate thickness

E_{LAM} = longitudinal modulus of the original laminate

E^* = longitudinal modulus of the delaminated laminate

The G in equation (1) depends on the layup and the location of the delaminated interfaces (which determines E^*), but does not depend on delamination size. If the undirectional lamina properties E_{11}, E_{22}, ν_{12}, and G_{12} are known, then E_{LAM} and E^* can be calculated from laminated plate theory and the rule of mixtures [5]. The $[\pm 30/\pm 30/90/\overline{90}]_s$ laminate originally proposed for measuring interlaminar fracture toughness [5,6,7] delaminates at the -30/90 interfaces. After delamination, this layup is modeled as three sublaminates, two $[\pm 30]_2$ laminates and one $[90]_3$ laminate, to account for the loss in compatibility of transverse contraction as delaminations grow under an applied strain. Thus,

$$E^* = \frac{8E_{(\pm 30)} + 3E_{(90)}}{11} \tag{2}$$

where $E_{(90)}$ is equal to E_{22}, and $E_{(\pm 30)}$ can be calculated either from laminated plate theory or measured from a tensile test of a $(\pm 30)_{ns}$ laminate [7]. In the $[\pm 35/0/90]_s$ layup, recently proposed as an alternate for use in the EDT test [8,9], delaminations grow between 0/90 interfaces. Hence,

this layup is modeled as three sublaminates, two $[\pm 35/0]_s$ laminates and one $[90]_2$ laminate. Thus,

$$E^* = \frac{6E_{(\pm 35/0)} + 2E_{(90)}}{8} \tag{3}$$

where again $E_{(90)}$ is equal to E_{22}, and $E_{(\pm 35/0)}$ may be calculated either from laminated plate theory or measured from a tensile test of a $(\pm 35/0)_s$ laminate. However, assuming the $(\pm 35/0)$ sublaminate is symmetric may lead to a small error in E^* because of the bending-extension coupling for this layup. The axial modulus of an asymmetric layup may be calculated from lami-- nated plate theory by assuming N_y, N_{xy}, κ_x, M_y, and κ_{xy} are all zero for a constant ε_x [10,11]. This technique allows for a nonzero κ_y and yields a slightly different axial modulus than is calculated for a $(\pm 35/0)_s$ laminate. This technique was used throughout this study to analyze G. The influence of bending-extension coupling on strain energy release rates is discussed further in appendix A.

Previously, delamination onset strains have been substituted into equation (1) to calculate the interlaminar fracture toughness. However, equation (1) assumes that the delamination growth is due only to the applied mechanical strain, ε^M. Theoretically, however, residual thermal stresses and the stresses due to absorbed moisture may contribute to the strain energy released as the delamination grows. Therefore, a new analysis was developed to account for these thermal and moisture influences.

Figure 1 shows a simplified model of a composite laminate containing a delamination of size "a" growing from either edge. The laminate is assumed to be typical of the layups previously used for the edge delamination test, with a set of n 90° plies in the center, and some combination of angle plies

and/or 0° plies on either side. Delaminations are assumed to occur at the interfaces between the central 90° plies and the neighboring angle plies. The laminated, LAM, and delaminated regions, SUB and $(90)_n$, are modeled as separate laminates loaded in parallel. The strain energy U is a function of delamination size, a, and may be written as the sum of the strain energy of three regions: the laminated portion, the separated 90_n°-ply group, and the separated sublaminates on either side of the 90_n° plies. Hence,

$$U(a) = U_{LAM}(a) + U_{SUB}(a) + U_{90}(a) \tag{4}$$

For any particular region, the strain energy may be defined in terms of strain and stress tensors as

$$U = \frac{1}{2} \int_V \varepsilon_{ij} \sigma_{ij} dV \tag{5}$$

The assumptions of classical laminated plate theory [12] may be used to redefine the strain energy as

$$U = \frac{w\ell}{2} \sum_{k=1}^{N} \int_{z_{k-1}}^{z_k} \{\varepsilon\}' \{\sigma\} dz \tag{6}$$

where $\{\varepsilon\}'$ represents the transpose of the strain vector and N is the total number of plies in the laminate or sublaminate. This formulation implicitly accounts for the midplane extension as well as the linear variation in stress and strain within each ply arising from out-of-plane bending. For a laminate experiencing no bending and having equal ply thicknesses h, equation (6) reduces to

$$U = \frac{w\ell\, t}{2} \frac{1}{N} \sum_{k=1}^{N} \{\varepsilon\}_k' \{\sigma\}_k \tag{7}$$

For an asymmetric laminate in uniaxial tension, however, there may be bending-extension coupling which requires the inclusion of pure bending and coupling terms in the expression for the strain energy. The derivation of these bending-extension coupling terms is presented in appendix A. Equation (7) may be rewritten as

$$U = w\ell t\, u \tag{8}$$

where u is the strain energy density defined as

$$u = \frac{1}{2N} \sum_{k=1}^{N} \{\varepsilon\}_k' \{\sigma\}_k \tag{9}$$

For the model shown in figure 1, $w_{LAM} = 2(b-a)$, $w_{sub} = 2a$, and $w_{90_n} = 2a$. Combining these expressions with equations (4) and (8) yields the following equations:

$$U(a) = 2\ell[(t_{SUB}u_{SUB} + t_{90}u_{90} - t_{LAM}u_{LAM})a + (t_{LAM}u_{LAM})b] \tag{10}$$

The strains in equations (6), (7), and (9) are total strains consisting of the sum of a mechanical, thermal, and hygroscopic term. Hence, the total strain may be written as

$$\{\varepsilon\}_k = \{\varepsilon\}_k^M + \{\varepsilon\}_k^T + \{\varepsilon\}_k^H \tag{11}$$

The mechanical component is simply the uniaxial nominal strain, i.e.,

$$\{\varepsilon\}_k^M = \begin{Bmatrix} \varepsilon^o \\ 0 \\ 0 \end{Bmatrix} \tag{12}$$

The residual thermal strains are given by the following:

$$\{\varepsilon\}_k^T = \begin{Bmatrix} \bar{\alpha}_x - \alpha_x^k \\ \bar{\alpha}_y - \alpha_y^k \\ \bar{\alpha}_{xy} - \alpha_{xy}^k \end{Bmatrix} \Delta T \tag{13}$$

where $\bar{\alpha}$ is the coefficient of thermal expansion of the region,

α^k is the coefficient of thermal expansion of the k^{th} ply in the region, and

ΔT is the difference between the stress-free cure temperature and the temperature of the ambient environment in which the laminate is tested.

However, for the sublaminates and the $(90)_n$-ply group, $\bar{\alpha}_x$ becomes $\bar{\alpha}_x$ of the original laminate because the delaminated regions are constrained by the grips to the original laminates' free thermal expansion.[1]

The hygroscopic (moisture) strains are given by

$$\{\varepsilon\}_k^H = \begin{Bmatrix} \bar{\beta}_x - \beta_x^k \\ \bar{\beta}_y - \beta_y^k \\ \bar{\beta}_{xy} - \beta_{xy}^k \end{Bmatrix} \Delta H \tag{14}$$

where $\bar{\beta}$ is the coefficient of moisture expansion of the region,

β_x^k is the coefficient of moisture expansion of the k^{th} ply in the region, and

ΔH is the percent weight difference of the laminate between the time of testing and the dry condition.

[1]This restriction applies only to the longitudinal strains, ε_x, and not to the transverse, ε_y, and shear strains, γ_{xy}.

However, for the sublaminates and the $(90°)_n$-ply group, $\bar{\beta}_x$ becomes $\bar{\beta}_x$ of the original laminate because the delaminated regions are constrained by the grips to the original laminate free moisture expansion.[1]

The laminar stresses in equations (6), (7), and (9) are calculated from strains of equation (11) as,

$$\{\sigma\}_k = [\bar{Q}]_k \{\varepsilon\}_k$$

where $[\bar{Q}]_k$ is the transformed reduced stiffness matrix of the k^{th} ply as defined in reference 12.

Recall that for an elastic body containing a planar flaw of area, A, that extends under a constant remote strain ε, no external work is performed as the flaw extends, and hence the strain energy release rate may be written simply as

$$G = -\frac{dU}{dA} \tag{15}$$

For the delaminated laminate modeled in figure 1, $A = 2\ell a$. Hence, $dA = 2\ell\, da$, and

$$G = -\frac{1}{2\ell}\frac{dU}{da} \tag{16}$$

Substituting equation (10) into equation (16) and differentiating yields

$$G = t_{LAM}u_{LAM} - t_{SUB}u_{SUB} - t_{90}u_{90} \tag{17}$$

where u for each region is given by equation (9). Therefore, the strain energy release rate analysis requires a ply-by-ply evaluation of the strain energy in the laminated and delaminated regions to account for the biaxial thermal residual and moisture stresses that may be present in the laminate as delaminations grow.

Figure 2 shows the influence of residual thermal and moisture stresses on the strain energy release rate associated with edge delamination growth in the -30°/90° interfaces of the 11 ply $[\pm 30/\pm 30/90/\overline{90}]_s$ laminate. The arrow pointing to the -30/90 interface in the figure caption indicates the delaminated interface. Graphite-epoxy lamina properties from reference 13 were used in the analysis, along with the following thermal and moisture coefficients [14]

$\alpha_1 = (-.23\ \mu\varepsilon/°F)\ -0.41\ \mu\varepsilon/°C$

$\alpha_2 = (14.9\ \mu\varepsilon/°F)\ 26.8\ \mu\varepsilon/°C$

$\beta_1 = 0$

$\beta_2 = 5560\ \mu\varepsilon/\text{weight percent}$

A mechanical strain of $\varepsilon = 0.01$ and a room temperature condition of 70°F were assumed. Therefore, ΔT was -280°F for the 350°F cured graphite-epoxy laminate. The ply thickness was assumed to be 0.0054 inch. As shown on the ordinate of figure 2, the strain energy release rate due to mechanical loading only, G^M, calculated from equation (17) is identical to the value calculated from equation (1). If the residual thermal strain is included, the strain energy release rate, G^{M+T}, is higher than G^M for the same applied strain. However, if the laminate absorbs moisture, the residual thermal stresses are relaxed and the strain energy release rate, G^{M+T+H}, decreases depending on the percentage of moisture weight gain, ΔH. For the case shown in figure 2, a moisture weight gain of 0.73 percent completely relaxes the residual thermal stresses, and the strain energy release rate, G^{M+T+H}, is equal to G^M where only mechanical strains were considered.

Figure 3 shows a similar relationship for delamination growth in the -45/90 interfaces of an 8 ply $[+45/0/-45/90]_s$ laminate. As previously shown in figure 2, the strain energy release rate for mechanical loading, G^M,

increases when residual thermal stresses are included, G^{M+T}, but decreases when moisture stresses are included, G^{M+T+H}.

Previously [5,6,8,11], the strain energy release rate calculated from equation (1) was shown to be equal to the sum of the G_I (interlaminar tension) and G_{II} (interlaminar shear) components calculated using a quasi-three-dimensional finite element analysis [15]. Like the total G, the G_I and G_{II} components were independent of delamination size; however, the percentage of the total G attributed to each component depended on the layup [6,8]. In order to determine the accuracy of equation (17) and determine the influence of residual thermal and moisture stresses on the individual fracture modes, the finite element analysis was modified.

Finite Element Analysis

In the quasi-three-dimensional analysis (Q3D) finite element analysis, the laminate is assumed to be long in the x-direction, and every x = constant plane deforms exactly in the same fashion as any other x = constant plane. Therefore, the gradients of displacements, strains, and stresses, with respect to the x coordinate are zero [15-18], and only one x = constant plane must be analyzed. Figure 4(a) shows such an x = constant plane. Because of symmetries in the problem, only one quadrant, defined by $0 \leq y \leq b$, $0 \leq z \leq t/2$, was analyzed. This region was modeled by eight-noded isoparametric elements. No singularity elements were used near the delamination front. Figure 4(b) shows a finite element model used for this analysis. The mesh consisted of 1271 nodes and 386 elements for analysis of the $[35/-35/0/90]_s$ laminate. The eight-noded elements at the delamination front were square, with the dimensions of each side equal to one fourth of a ply thickness. Strain energy release rates were calculated using the virtual crack extension technique [19].

The Q3D delamination problem was solved for three separate loading conditions: mechanical, thermal, and hygroscopic. For mechanical loading, the Q3D analysis is documented in references 16-18. For the thermal and hygroscopic loading the Q3D analysis was performed as presented in appendix B. The forces and displacements in the vicinty of the delamination front for the combined loading conditions of M+T, and M+T+H, were obtained by appropriate superposition of the forces and displacements for the M, T, and H, loading conditions. The combined forces and displacements were then used to calculate the components of the strain energy release rates G_I, G_{II}, and G_{III}. The sum of three components yielded the total G.

Inclusion of the thermal and moisture terms results in a coupled problem because of the coupling of the mechanical, thermal, and hygroscopic contributions to the strain energy released. Therefore, G results could not be normalized by a single loading term such as ε^2, ΔT, or ΔH. Hence, the results were presented for specific strain levels, at a ΔT of -280°F, for a range of moisture contents, ΔH.

Figure 5 compares the finite element results to the laminate plate theory results of figure 2 for delamination in the -30/90 interfaces of the eleven-ply $[\pm 30/\pm 30/90/\overline{90}]_s$ laminate. The laminate plate theory results from equation (17) agree well with the finite element results. Also shown in figure 5 is the G_I component of the total G calculated from the finite element analysis. A similar trend of the strain energy release rate due to mechanical loading, G_I^M, increasing when residual thermal stresses are included, G_I^{M+T}, and then decreasing with increasing moisture content, G_I^{M+T+H}, is apparent. The G_I component remained a fixed percentage of the total G for all the conditions analyzed. Figure 6 compares the finite element results to the laminate plate theory results from figure 3 for delamination in the -45/90 interfaces of the eight-ply $[45/0/-45/90]_s$ laminate. Again, the laminate plate theory and finite element analysis agree, and the G_I component is a fixed percentage of the total G for all the conditions analyzed. However, as the following discussion will illustrate, the G_I component may change with moisture content for other layups.

In reference 8, a family of laminates was evaluated where the total strain energy release rates for a remote mechanical strain were nearly identical, but the G_I percentage varied widely. The three layups examined were $[45/-45/0/90]_s$, $[45/0/-45/90]_s$, and $[0/45/-45/90]_s$. A small difference in total G was calculated for delaminations in $[45/-45/0/90]_s$ and

$[0/45/-45/90]_s$ laminates compared to the $[45/0/-45/90]_s$ laminate because of the curvature effect ($\kappa_y \neq 0$) on sublaminate moduli for the asymmetric laminates formed in the first two cases. This curvature effect on moduli is a consequence of the non-zero B_{11} and B_{22} terms in the [B] matrix influencing the longitudinal modulus. In the third case, the [45/0/-45] sublaminate has non-zero B_{16} and B_{26} terms only, corresponding to twist-extension coupling. These terms do not affect the longitudinal modulus of the sublaminate. Therefore, this sublaminate may be assumed to be symmetric. Assuming delaminations occurred between the 90° plies and the adjacent angle plies, equation (1) indicated that G^M was nearly identical for all three layups. However, the finite element analysis showed that these three layups had relatively high, intermediate, and low G_I^M percentages, respectively. Figure 7 shows the G_I component, normalized by the total G as a function of percent moisture weight gain for the three layups. All calculations were performed using the delamination onset strains for the appropriate laminates as measured in reference [8]. The solid symbols show the relative ratio of G_I to G for the three layups when mechanical strain only is considered. If residual thermal stresses are included in the analysis, the G_I/G ratios change for the $[45/-45/0/90]_s$ and $[0/45/-45/90]_s$ layups, but do not change for the $[45/0/-45/90]_s$ layups, as shown by the points labeled M+T on the ordinate. Furthermore, the G_I/G ratios continue to change for the first two layups as moisture content increases, but G_I/G remains unchanged with increasing ΔH for the third layup, as shown by the curves labeled M+T+H.

Figure 8 shows similar results for $[35/-35/0/90]_s$, $[35/0/-35/90]_s$, and $[0/35/-35/90]_s$ laminates assuming a mechanical strain of 0.00254. These layups were chosen for the edge delamination test based on a parametric study

to minimize the delamination onset strain required to measure the interlaminar fracture toughness of a given material [8]. As was the case for the family of quasi-isotropic layups studied, the only layup of the three that maintained a constant G_I/G ratio when thermal and moisture effects where included was the $[35/0/-35/90]_s$ layup that had $(\theta/0/-\theta)$ sublaminates after delamination. Apparently, layups that form asymmetric sublaminates when they delaminate have G_I and G_{II} components that vary with ΔH. For these layups, delamination is driven by a combination of Poisson mismatch of the individual plies and a curvature effect due to bending-extension coupling. However, layups that form symmetric sublaminates (or laminates that are asymmetric only in the sign of the angle plies) after delamination maintain constant G_I/G ratios as moisture content changes. For these laminates, delamination is driven entirely by Poisson mismatch.

Figure 9 shows that the G_I/G ratio also changes with the level of mechanical strain. The variation in G_I/G with ΔH is much greater as low strain levels than at higher strains. Therefore, the influence of thermal and moisture stresses on mixed-mode ratios will not be as significant for tough materials that delaminate at relatively high strains as it may be for more brittle materials that delaminate at lower strains.

Experiments

Specimen Preparation

An experimental program was conducted to determine the relative significance of including residual thermal and moisture stresses in strain energy release rate analysis for interlaminar fracture toughness measurement. First, a 0.093 m^2 (1 ft^2) panel of T300/5208 graphite-epoxy was fabricated from prepreg tape. The $[\pm 35/0/90]_s$ layup was chosen to maximize the mode I contribution and minimize the possibility of extensive 90°-ply cracking occurring before delamination onset [8]. The panel was cured and cooled overnight while still under pressure in the vacuum bag in the autoclave. The next morning the panel was removed and was immediately cut, using a diamond saw, into 44 specimens, 127 mm (5 in.) long by 12.7 mm (0.5 in.) wide.[4] Each specimen was immediately weighed to the nearest 0.001 gram. Of the 44 specimens, 4 were tested immediately in the "aftercured condition," 4 were stored in a desiccator, 11 were dried in a vacuum oven at 100°C, 8 were soaked in water, and the remainder were stored in ambient laboratory air. Specimens were chosen from a variety of panel positions for each condition. The percentage moisture weight gain was monitored for each condition for approximately 2 months until the specimen weight stabilized. For example, figure 10 shows the measured moisture weight gain for the specimens that were soaked in water. A final specimen weight was measured just before testing.

Specimens dried in the vacuum oven at 100°C for one month between the time they were cut and when they were tested showed an average moisture weight

[4]Because the specimens had to be weighed to determine moisture weight gain, the specimen dimensions had to be much less than the 254 mm (10 in.) by 38.1 mm (1.5 in.) size used previously [5-9]. A recent study indicated that EDT specimen size did not affect measured delamination onset strains. Therefore, an optimum size was chosen that was small enough to weigh but large enough to instrument with a 25.4 mm (1 in.) gage length extensometer.

loss of 0.21 percent. Therefore, an 0.21 percent weight gain was added to the ΔH measured for each condition to approximate the percentage moisture weight gain from a truly dry state (table 1).

Modulus Measurement

The thickness of each specimen was recorded at three positions along the length of each specimen, near either edge, and averaged. Axial strain was measured with a 25.4 mm (1.0 in.) extensometer centered over a 76.2 mm (3.0 in.) gage length. The blades of the extensometer rested in "V" shaped grooves cut into thin aluminum plates that were mounted on the specimen with a fast drying adhesive. Load and strain data were recorded on an x-y recorder. Table 1 shows the average thickness and modulus measured for the specimens tested. Although the average modulus varied somewhat with ΔH, only the water-soaked case showed significant variation. Therefore, a single set of lamina properties were used to calculate E_{LAM} and E^* in equation (1), and to calculate strain energy release rates for all but the saturated case.

The following properties were measured for T300/5208 undirectional lamina at room temperature under ambient conditions:

E_{11} = 18.7 Msi (128 GPa)

E_{22} = 1.23 Msi (8.47 GPa)

G_{12} = 0.832 Msi (5.73 GPa)

ν_{12} = 0.292

An axial laminate modulus of 9.08 Msi (62.5 GPa) was calculated for the $[35/-35/0/90]_s$ layup from laminated plate theory using these properties. This calculated modulus was close to the average measured modulus (excluding the water-soaked case) of 9.05 Msi (62.4 GPa). The delaminated modulus, E^*, calculated for delamination in the 0/90 interfaces of the $[35/-35/0/90]_s$ laminate was 7.61 Msi (52.4 GPa). In order to simulate the modulus reduction

in the water-soaked case, E_{11} was reduced to 18.1 Msi (125 GPa). This yielded an axial laminate modulus of 8.83 Msi (60.8 GPa) which was the same as the measured value. The corresponding value of E^* for the water-soaked case was 7.44 Msi (51.3 GPa).

Edge Delamination Tests

For all specimens, an abrupt deviation in the linear load-deflection curve ocurred when delaminations formed on the edge. Delamination onset strains, ε_c, for each moisture condition are shown in figure 11. Mean values of ply thickness, delamination onset strain, and measured moisture weight gain for each condition (shown in table 2) were substituted into equation (17) to calculate G_c^{M+T+H}. A ΔT of -280°F was assumed because it represents the largest gradient possible for tests conducted at room temperature.

Figure 12 shows G_c^{M+T+H} values plotted as a function of percentage moisture weight gain. Also shown in figure 12 are G_c^M values calculated from equation (17) using the average delamination onset strains for each condition. The G_c^{M+T+H} values do not agree with the G_c^M values, with differences of the order of thirty percent occurring for the vacuum-dried case ($\Delta H = 0\%$) and the water-soaked case ($\Delta H = 1.55\%$). For the ambient condition ($\Delta H = 0.52\%$), however, the G_c^{M+T+H} and G_c^M values were within twelve percent of each other because the moisture contribution nearly cancelled the residual thermal contribution to G.

In addition to comparing the total G_c, the mode I component was plotted and compared because previous work had indicated that composites with brittle epoxy matrices delaminate under interlaminar tension and are insensitive to the presence of interlaminar shear [8,9]. The appropriate mode I percentage of the total G_c shown in table 2 was determined from the finite element analysis for the measured ε_c and ΔH (assuming a ΔT of -280°F), and was

used to calculate G_{Ic} (fig. 13). Figure 13 shows the difference between G_{Ic} values where thermal and moisture effects have been included and G_{Ic} values where they have been neglected. There is less difference between G_{Ic}^{M} and G_{Ic}^{M+T+H} values than was observed for the total G_c measurements. At the ambient conditions ($\Delta H = 0.52\%$), the difference was only seven percent. Hence, for most practical purposes, residual thermal and moisture effects may be neglected for interlaminar fracture toughness measurements under ambient conditions. However, the dry and water-soaked laminates showed significant differences in both G_c and G_{Ic} values using the two analyses (figs. 12 and 13). Therefore, thermal and moisture effects may need to be included for G analysis of composites tested under dry or hot-wet conditions. Furthermore, toughened composites containing thermoplastic matrices that are manufactured at very high temperatures, but absorb very little moisture, may require inclusion of residual thermal and moisture effects to accurately predict G values because they may have relatively low moisture contents with relatively high ΔT values. However, as was shown in figure 9, thermal and moisture effects become less dominant for toughened-matrix composites that delaminate at high strain levels, because the mechanical strain has the greatest contribution to the strain energy released.

Discussion

The significance of residual thermal and moisture stresses to strain energy release rates ultimately depends on how these measurements are used. If toughness measurements are used to compare materials for improved delamination resistance, then these thermal and moisture effects become of secondary importance. This is especially true if tests are conducted at room-temperature ambient conditions, and the difference in toughness measurements for different materials is large [4,5,6]. For example, a seven percent error

in G_{Ic} due to neglecting thermal and moisture effects for the $[\pm 35/0/90]_s$ EDT tests is insignificant compared to a ten-fold increase in G_{IC} for composites with toughened matrices.

If, however, these interlaminar toughness measurements are used as delamination failure criteria to predict delamintion growth in composite structures of the same material, but with different geometries and loadings, then these thermal and moisture effects may become more significant. Other factors may need to be addressed to accurately calculate G. For example, the coefficient of thermal expansion may not be constant between the cure temperature and room temperature. In addition, assuming that the average moisture content of the laminate is representative of the moisture content at the delamination front may also be in error. Some knowledge of the moisture distribution through the laminate may be needed. The detailed information required for carefully conducted laboratory tests may not be available to analyze the strain energy release rate for the delamination growing in the structure. Nevertheless, conducting edge delamination tests where these effects can be quantified, and compared to data from other interlaminar fracture toughness tests where these effects are not present, would help document the relative significance of residual thermal and moisture stresses on the interlaminar fracture of composite materials.

Conclusions

Based on the analyses and experiments performed during this study, the following conclusions have been reached:

(1) The strain energy release rate calculated for edge delamination growth at a constant ΔT increases when residual thermal stresses are included with applied mechanical strains, but decreases when these residual stresses are relaxed with increasing moisture content.

(2) When residual thermal and moisture stresses are included in strain energy release rate analyses, the ratio of G_I to G is constant for laminates modeled as symmetric sublaminates after delamination, but for laminates modeled as asymmetrical sublaminates after delamination the G_I/G ratio changes with moisture content and mechanical strain.

(3) For graphite-epoxy composites residual thermal and moisture stresses do not significantly alter the calculation of interlaminar fracture toughness from strain energy release rate analysis of edge delamination data taken at room temperature and ambient moisture conditions. However, for epoxy-matrix composites tested under dry or hot/wet conditions the influence of residual thermal and moisture stresses may need to be considered to accurately predict strain energy release rates for edge delamination.

Appendix A

This appendix presents the formulation of the bending, extension, and coupling terms included in the expressions for strain energy of a laminate. The strain energy of a given volume may be defined in terms of strain and stress tensors as

$$U = \frac{1}{2}\int_V \varepsilon_{ij}\sigma_{ij}\, dV \tag{A1}$$

If the volume is composed of orthotropic laminae and is in a state of plane stress, the assumptions of laminated plate theory may be used to redefine the strain energy in terms of the engineering stress and total strain vectors in the laminate coordinate system (x,y,z) as

$$U = \frac{w\ell}{2}\sum_{k=1}^{N}\int_{z_{k-1}}^{z_k} \{\varepsilon\}' \{\sigma\}\, dz \tag{A2}$$

For the general case in which extension and bending occur, the total strain at any point is given by the sum of the mid-plane strain and the product of the curvature and the distance from the mid-plane

$$\{\varepsilon\} = \{\varepsilon^o\} + z\{\kappa\} \tag{A3}$$

The mid-plane strain and curvature are each composed of mechanical, M, thermal, T, and hygroscopic (or moisture), H, components, and may be written as

$$\{\varepsilon^o\} = \{\varepsilon^o\}^M + \{\varepsilon^o\}^T + \{\varepsilon^o\}^H = \{\varepsilon^o\}^M + \{\bar{\alpha}\}\Delta T + \{\bar{\beta}\}\Delta H$$

$$\{\kappa\} = \{\kappa\}^M + \{\kappa\}^T + \{\kappa\}^H = \{\kappa\}^M + \{\bar{\lambda}\}\Delta T + \{\bar{\mu}\}\Delta H \tag{A4}$$

where $\{\bar{\alpha}\}$ and $\{\bar{\beta}\}$ are, respectively, the laminate coefficients of thermal and moisture expansion and $\{\bar{\lambda}\}$ and $\{\bar{\mu}\}$ are, respectively, the laminate

coefficients of thermal and moisture curvature. These vectors are defined as follows:

$$\begin{Bmatrix} \bar{\alpha} \\ \bar{\lambda} \end{Bmatrix} = \frac{1}{\Delta T} \begin{bmatrix} A & B \\ B & D \end{bmatrix}^{-1} \begin{Bmatrix} N \\ M \end{Bmatrix}^{T}, \quad \begin{Bmatrix} \bar{\beta} \\ \bar{\mu} \end{Bmatrix} = \frac{1}{\Delta H} \begin{bmatrix} A & B \\ B & D \end{bmatrix}^{-1} \begin{Bmatrix} N \\ M \end{Bmatrix}^{H}. \tag{A5}$$

The force and moment resultants, $\{N\}$ and $\{M\}$, are related to the mid-plane strain and curvature by

$$\begin{Bmatrix} N \\ M \end{Bmatrix} = \begin{bmatrix} A & B \\ B & D \end{bmatrix} \begin{Bmatrix} \varepsilon^{o} \\ \kappa \end{Bmatrix} \tag{A6}$$

where the load and moment are each composed of mechanical, thermal, and hygroscopic components as follows:

$$\begin{aligned} \{N\} &= \{N\}^{M} + \{N\}^{T} + \{N\}^{H} = \{N\}^{M} + \Delta T \sum_{k=1}^{N} [\bar{Q}]_k \{\alpha\}_k t_k \\ &\quad + \Delta H \sum_{k=1}^{N} [\bar{Q}]_k \{\beta\}_k t_k \\ \{M\} &= \{M\}^{M} + \{M\}^{T} + \{M\}^{H} = \{M\}^{M} + \Delta T \sum_{k=1}^{N} [\bar{Q}]_k \{\alpha\}_k (z_k^2 - z_{k-1}^2)/2 \\ &\quad + \Delta H \sum_{k=1}^{N} [\bar{Q}]_k \{\beta\}_k (z_k^2 - z_{k-1}^2)/2 \end{aligned} \tag{A7}$$

The stress in the k^{th} ply is given by the product of the transformed reduced stiffness matrix $[\bar{Q}]_k$, and mechanical strain of the ply, where the mechanical strain is the total strain less the free thermal and moisture strains of that ply

$$\{\sigma\}_k = [\bar{Q}]_k \left(\{\varepsilon\} - \{\alpha\}_k \Delta T - \{\beta\}_k \Delta H\right) \tag{A8}$$

here $\{\alpha\}_k$ and $\{\beta\}_k$ are the lamina coefficients of thermal and moisture expansion, respectively.

After substitutions of equations (A3) and (A8), evaluation of equation (A2) yields an expression for the strain energy of a laminate in terms of the strain energy densities of the individual plies

$$U = w\ell \sum_{k=1}^{n} t_k(u_{ek} + u_{ck} + u_{bk}) = w\ell \sum_{k=1}^{N} t_k u_k \tag{A9}$$

where

$$u_{ek} = \frac{1}{2} \{\varepsilon^o\}' [\bar{Q}]_k (\{\varepsilon^o\} - \{\alpha\}_k \Delta T - \{\beta\}_k \Delta H) \tag{A10}$$

is the strain energy density in the k^{th} ply derived strictly from extension,

$$u_{bk} = \frac{1}{6}(z_k^2 + z_k z_{k-1} + z_{k-1}^2) \{\kappa\}' [\bar{Q}]_k \{\kappa\} \tag{A11}$$

is the strain energy density in the k^{th} ply due to bending only, and

$$u_{ck} = \frac{1}{4}(z_k + z_{k-1})\{\kappa\}' [\bar{Q}]_k (2\{\varepsilon^o\} - \{\alpha\}_k \Delta T - \{\beta\}_k \Delta H) \tag{A12}$$

is the strain energy density in the k^{th} ply associated with coupling between extension and bending. Hence, for an asymmetric sublaminate, equations (A10) - (A12) would be summed in equation (A9), instead of using equation (A10) alone, to calculate strain energy density, u_{SUB}, and is used in the strain energy release rate calculation of equation (17). Figure 14 shows the influence of including equations (A11) and (A12) in the calculation of G^{M+T+H} for a $[\pm 35/0/90]_s$ laminate delaminated at the 0/90 interface. As moisture content exceeds 0.6 percent, G^{M+T+H} became significantly larger when coupling terms were included. The G_c values tabulated in table 2 were calculated with bending and coupling terms included.

Appendix B

This appendix presents the general formulation of the Q3D thermal loading analysis. The formulation used for the hygroscopic loading is similar and hence is not presented here.

Consider a laminate subjected to a temperature change of ΔT and no other loading. Due to this temperature change, each ply of the laminate tends to either expand or contract, but each ply is constrained by the neighboring ply. Therefore, in the interior of the laminate stresses consistant with laminated plate theory develop to maintain compatibility of deformation. Near free edges, however, interlaminar stresses develop to maintain compatibility. Because the laminate is long, every x = constant plane contracts or expands in exactly the same manner. However, the amount of this contraction or expansion is not known. But, because there is no other loading on the laminate, the net force in the x-direction must be zero. This condition was used to determine the amount of contraction or expansion in the x-direction (and hence the strain ε_x).

The thermal problem shown in figure 15(a), can be decomposed into two subproblems. In the first subproblem (fig. 15(b)) the laminate is subjected to a temperature change ΔT and constrained so that $\varepsilon_x = 0$. In the other subproblem (fig. 15(c)) there is no temperature change, but there is a uniform axial strain of $\varepsilon_x = 1$.

The subproblem in figure 15(c) is simply the mechanical load problem of references 15, 16 and 17. The total solution for the thermal problem in figure 15(a) is obtained by scaling the solution for the second subproblem figure 15(c) by the unknown axial strain ε_o and adding the solutions of the two subproblems together. Because the only loading for the problem shown in figure 15(a) is the temperature change, ΔT, the sum of the axial forces of

the two subproblems must be equal to zero. This leads to the following equation:

$$f_{x1} + \varepsilon_o f_{x2} = 0 \tag{B1}$$

which may be solved for the strain due to a temperature change as:

$$\varepsilon_o = - \frac{f_{x1}}{f_{x2}} \tag{B2}$$

References

1. Starnes, J. H., Rhodes, M. D., and Williams, J. G., "The Effect of Impact Damage and Circular Holes on the Compressive Strength of a Graphite-Epoxy Laminate," ASTM STP 696, 1979, pp. 145-171.
2. Williams, J. G., and Rhodes, M. D., "The Effect of Resin on the Impact Damage Tolerance of Graphite-Epoxy Laminates," ASTM STP 787, Composite Materials, Testing and Design (Sixth Conference), 1982, pp. 450-480.
3. Byers, B. A., "Behavior of Damaged Graphite/Epoxy Laminates Under Compression Loading," NASA CR 159293, August 1980.
4. Carlisle, D. R., and Leach, D. C., "Damage and Notch Sensitivity of Graphite/PEEK Composite," Proceedings of the 15th National SAMPE Technical Conference, October 1983, pp. 82-93.
5. O'Brien, T. K., "Characterization of Delamination Onset and Growth in a Composite Laminate," in Damage in Composite Materials, ASTM STP 775, June 1982, p. 140. (Also in NASA TM-81940, January 1981.)
6. O'Brien, T. K., Johnston, N. J., Morris, D. H., and Simonds, R. A., "A Simple Test for the Interlaminar Fracture Toughness of Composites," SAMPE Journal, Vol. 18, No. 4, July/August 1982, p. 8.
7. Johnston, N. J., O'Brien, T. K., Morris, D. H., and Simonds, R. A., "Interlaminar Fracture Toughness of Composites II - Refinement of the Edge Delamination Test and Application to Thermoplastics," Proceedings of the 28th National SAMPE Symposium and Exhibition, Anaheim, California, April 1983, p. 502.
8. O'Brien, T. K., "Mixed-Mode Strain-Energy-Release-Rate Effects on Edge Delamination of Composites," in "The Effect of Defects in Composite Materials," ASTM STP 836, 1984, pp. 125-142. Also in NASA TM-84592, January 1983.

9. O'Brien, T. K., Johnston, N. J., Morris, D. H., and Simonds, R. A., "Determination of Interlaminar Fracture Toughness and Fracture Mode Dependence of Composites Using the Edge Delamination Test," Proceedings of the International Conference on Testing, Evaluation, and Quality Control of Composites, University of Surrey, Guildford, England, September 1983, pp. 223-232.

10. Ho, T., and Schapery, R. A., "The Effect of Environment on the Mechanical Behavior of AS/3501-6 Graphite Epoxy Material--Phase IV, Naval Air Systems Command (ATC) Report No. R-92000/3CR-9, February 1983.

11. Whitcomb, J. D., and Raju, I. S., "Analysis of Interlaminar Stresses in Thick Composite Laminates With and Without Edge Delamination," NASA TM 85738, January 1984. (Presented at the ASTM Symposium on "Delamination and Debonding of Materials," Pittsburgh, PA, November, 1983.)

12. Jones, R. M., "Mechanics of Composite Materials," Scripta, McGraw-Hill, South Orange, NJ, 1975.

13. Rodini, B. T., Jr., and Eisenmann, J. R., "An Analytical and Experimental Investigation of Edge Delamination in Composite Laminates," Fibrous Composites in Structural Design, Plenum, New York, 1980, pp. 441-457.

14. Kriz, R. D., and Stinchcomb, W. W., "Effects of Moisture, Residual Thermal Curing Stresses, and Mechanical Load on the Damage Development in Quasi-Isotropic Laminates," in Damage in Composite Materials, ASTM STP 775, 1982, pp. 63-80.

15. Raju, I. S., and Crews, J. H., Jr., "Interlaminar Stress Singularities at a Straight Free Edge in Composite Laminates," Computers and Structures, Vol. 14, No. 1-2, 1981, pp. 21-28.

16. Pipes, R. B., and Pagano, N. J., "Interlaminar Stresses in Composite Laminates Under Uniform Axial Extension," Journal of Composite Materials, Vol. 4, October 1970, pp. 538-548.

17. Wang, A. S. D., and Crossman, F. W., "Some New Results on Edge Effects in Symmetric Composite Laminates," Journal of Composite Materials, Vol. 14, January 1977, pp. 92-106.

18. Wang, A. S. D., and Crossman, F. W., "Edge Effects on Laterally Thermally Induced Stresses in Composite Laminates," Journal of Composite Materials, Vol. 11, July 1977, pp. 300-312.

19. Rybicki, E. F., and Kanninen, M. F., "A Finite Element Calculation of Stress Intensity Factors by a Modified Crack Closure Integral," Engineering Fracture Mechanics, Vol. 9, 1977, pp. 931-938.

20. Parker, B. M., "The Effect of Composite Prebond Moisture on Adhesive Bonded CFRP-CFRP Joints," Composites, Vol. 14, No. 3, July 1983.

TABLE 1.- AVERAGE PHYSICAL PROPERTY MEASUREMENTS FOR T300/5208 $(\pm 35/0/90)_s$ LAMINATES

Environment	ΔH% From Cure	ΔH% From Dry	No. of Tests	t, in(mm)	E_{LAM}, M_{si} (GPa)
Vacuum Dried	-0.210	0.0	11	.0424 (1.077)	9.02 (62.1)
After Cured	0.0	.21	4	.0433 (1.100)	9.10 (62.7)
Dessicator	.112	.32	4	.0425 (1.080)	9.02 (62.2)
Ambient	.310	.52	14	.0427 (1.085)	9.08 (62.6)
Water Soaked	1.34	1.55	8	.0428 (1.087)	8.83 (60.9)

TABLE 2.- EDGE DELAMINATION DATA REDUCTION FOR CRITICAL STRAIN ENERGY RELEASE RATE

Environment	ΔH%	h, in(mm)	ε_c	G_c, $\left(\frac{\text{in-lbs}}{\text{in}^2}\right)$ KJ/M^2			
				G_c^M	G_c^{M+T+H}	G_{Ic}^M	G_{Ic}^{M+T+H}
Vacuum Dried	0.0	0.0053 (0.135)	0.00471	0.674 (0.118)	1.053 (0.185)	0.635 (0.111)	0.815 (0.143)
After Cured	.21	.0054 (.137)	.00465	.670 (.118)	.962 (.169)	.631 (.111)	.775 (.136)
Dessicator	.32	.0053 (.135)	.00493	.740 (.130)	.944 (.166)	.697 (.122)	.804 (.141)
Ambient	.52	.0053 (.135)	.00521	.825 (.145)	.937 (.164)	.777 (.136)	.838 (.147)
Water Soaked	1.55	.0054 (.137)	.00548	.866 (.152)	.628 (.110)	.816 (.143)	.621 (.109)

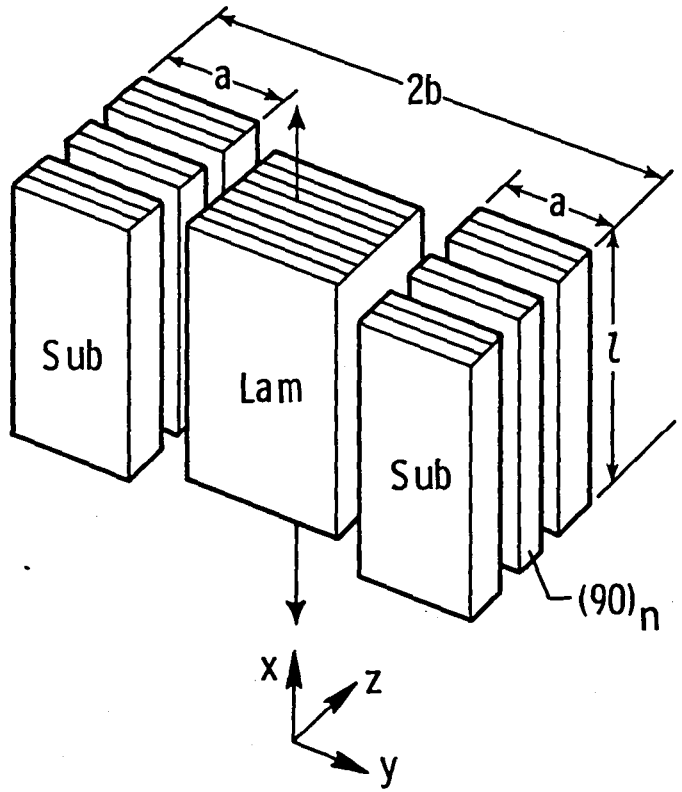

Fig. 1 Model of a partially delaminated composite laminate.

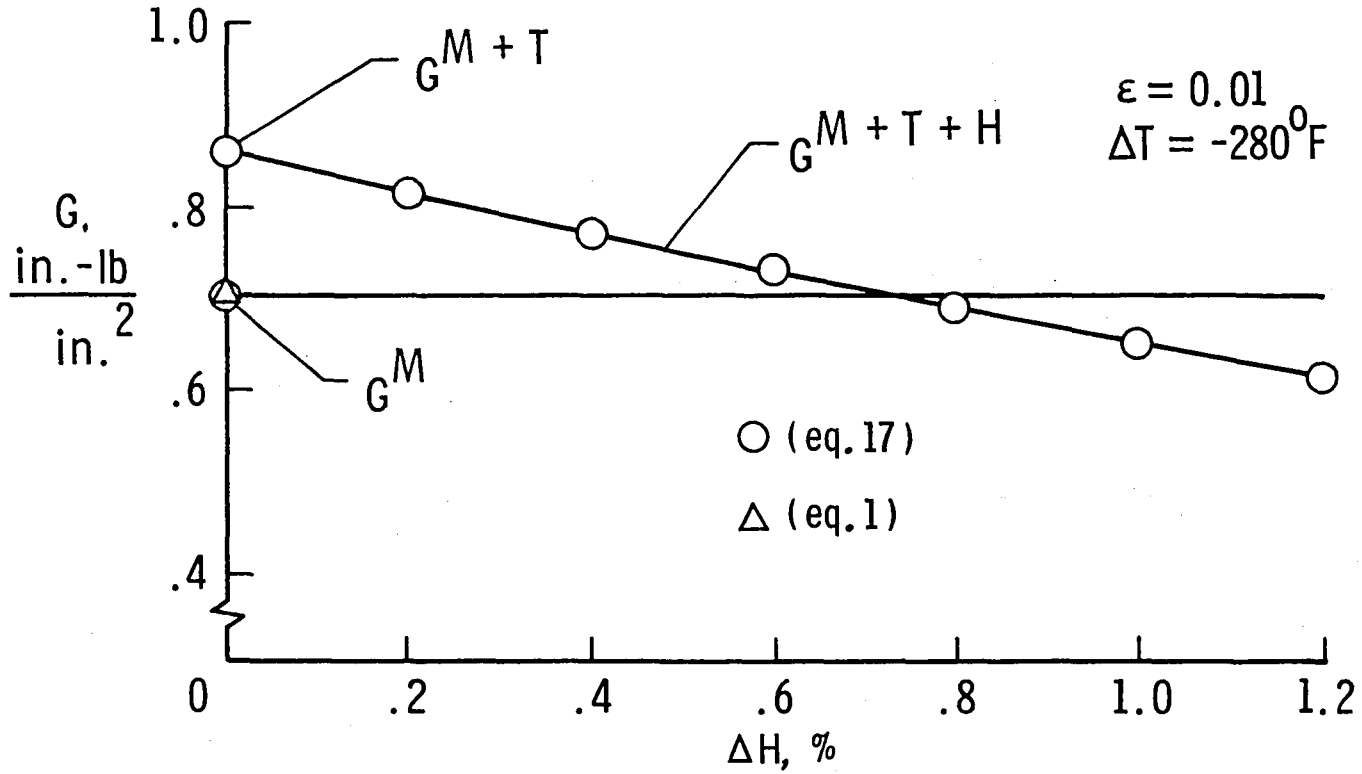

Fig. 2 Influence of residual thermal and moisture stresses on strain energy release rate $[\pm 30/\pm 30/90/\overline{90}]_s$ T300/5208.

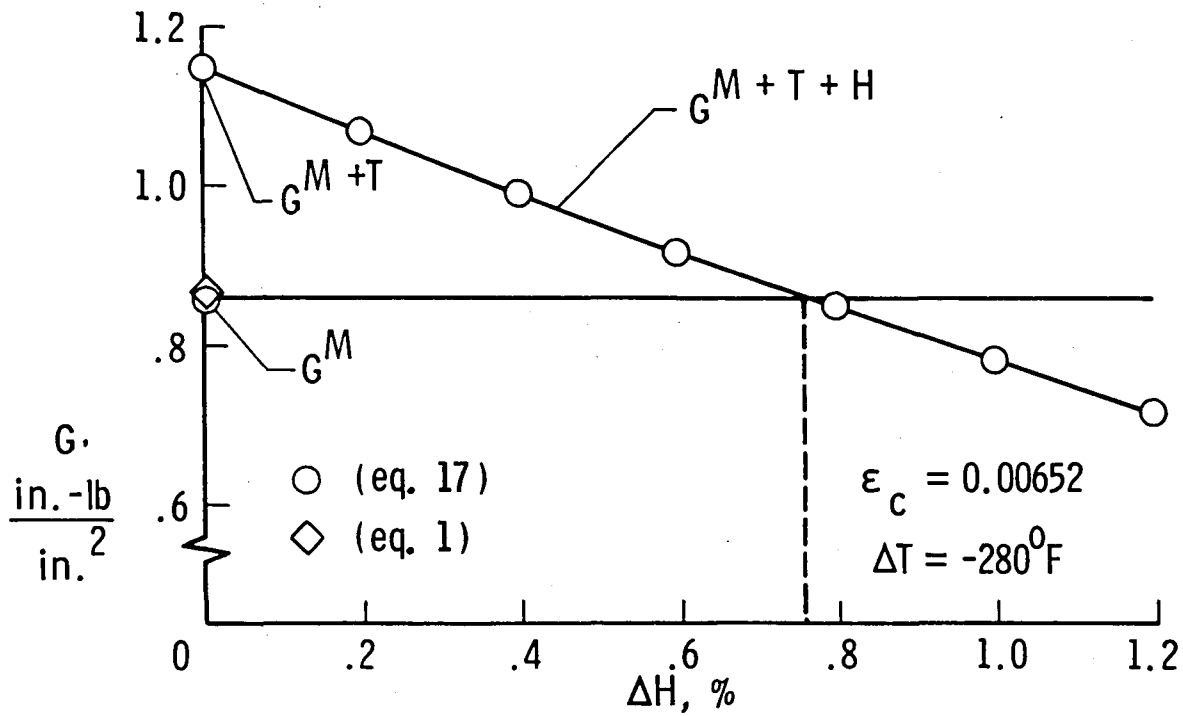

Fig. 3 Influence of residual thermal and moisture stresses on energy release rate $[45/0/-45/90]_s$ T300/5208.

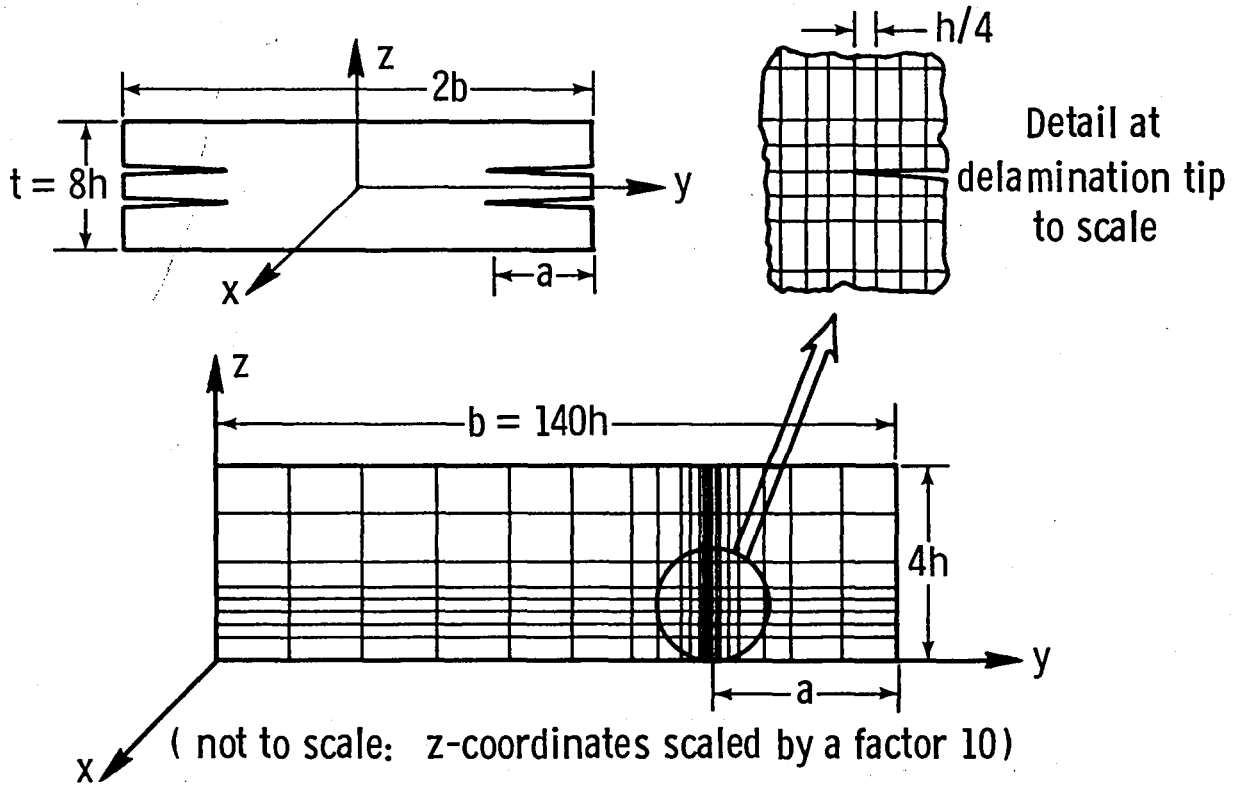

Fig. 4 Discretization of Laminate Cross Section for Finite Element Analysis

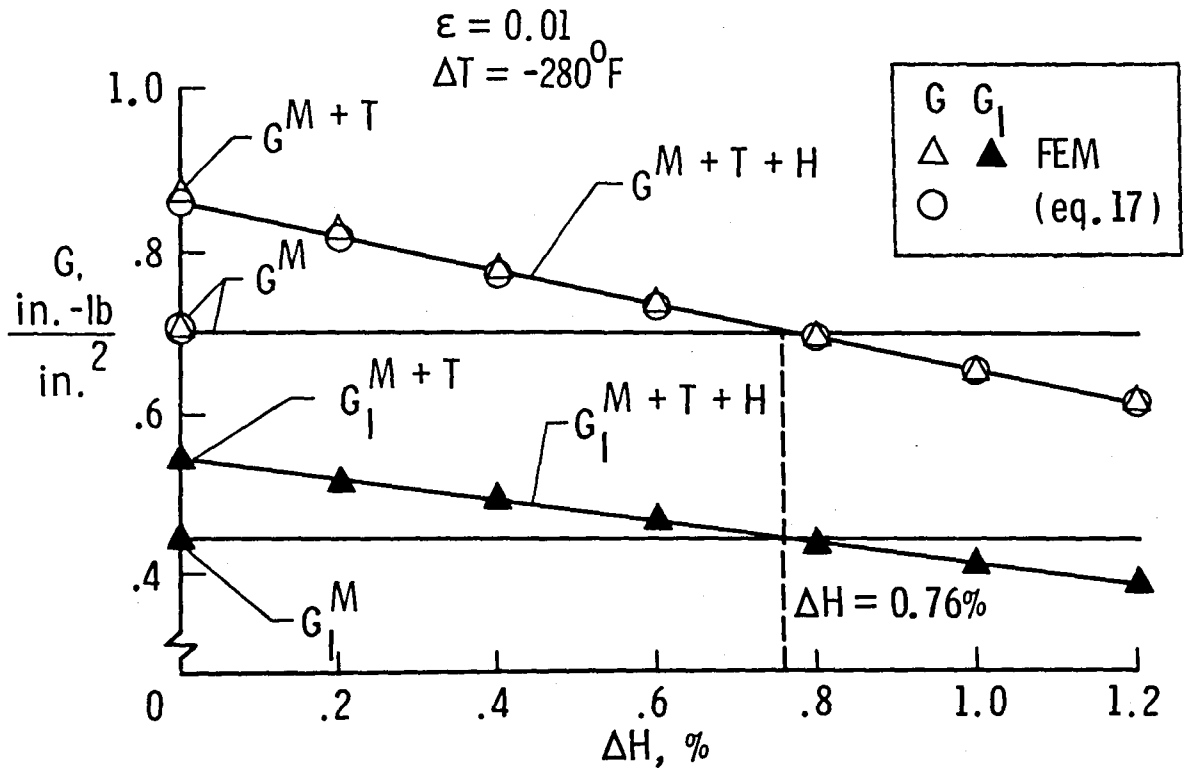

Fig. 5 Influence of residual thermal and moisture stresses on strain energy release rate components $[\pm 30/\underset{\uparrow}{\pm} 30/90/\overline{90}]$ T300/5208.

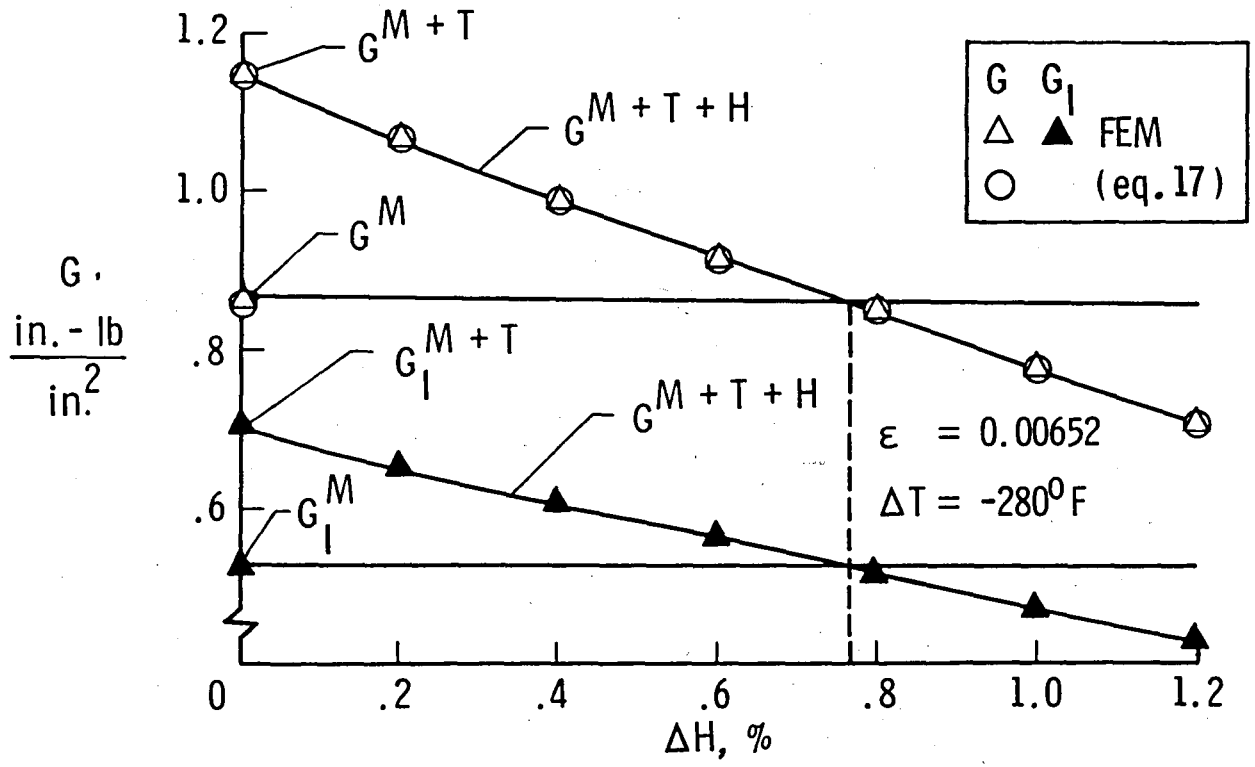

Fig. 6 Influence of residual thermal and moisture stresses on strain energy release rate components $[45/0/-45/90]_s$ T300/5208.

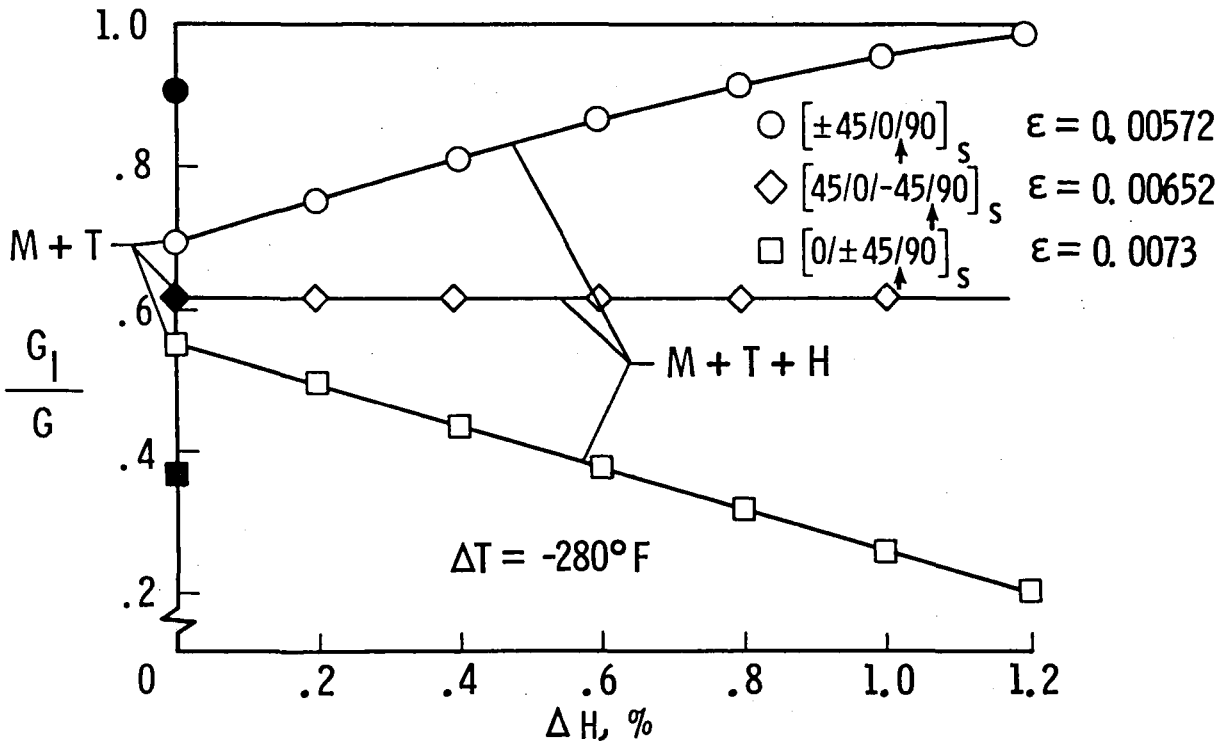

Fig. 7 Effect of residual thermal and moisture stresses on percentage Mode I strain energy release rate for quasi-isotropic laminate.

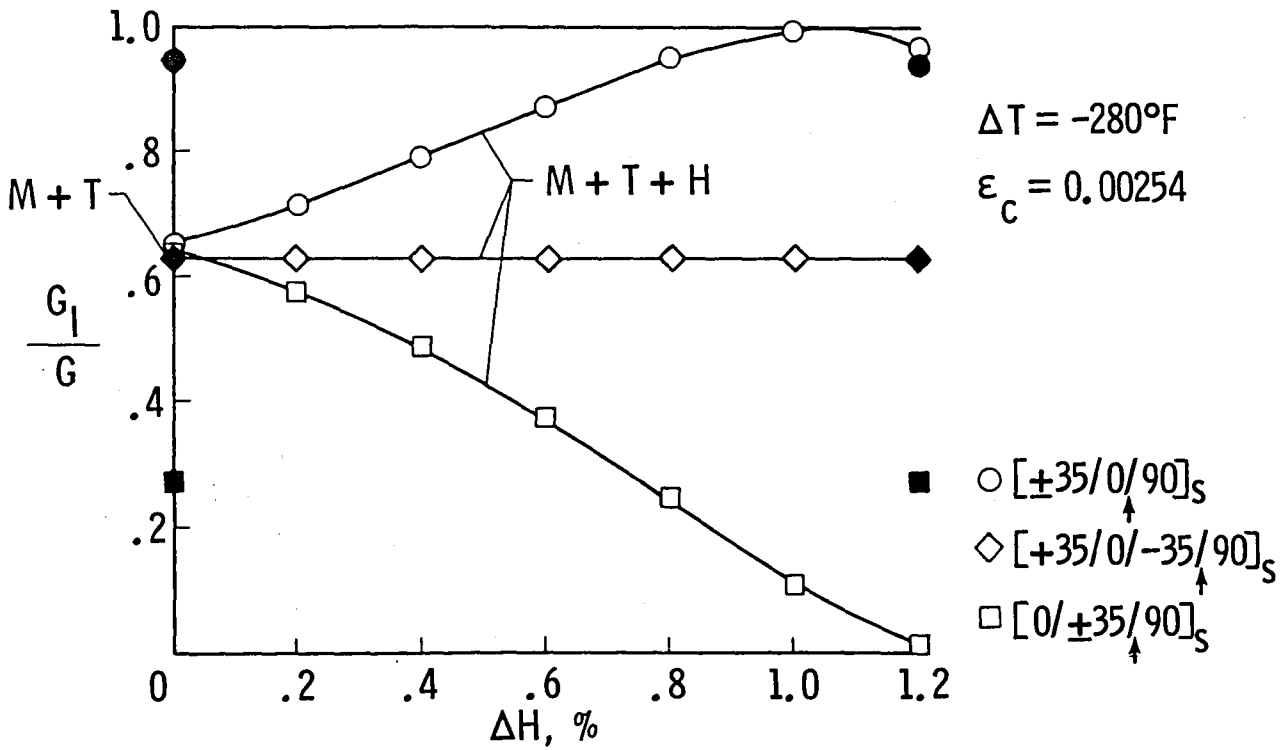

Fig. 8 Effect of residual thermal and moisture stresses on Mode I percentage strain energy release rate.

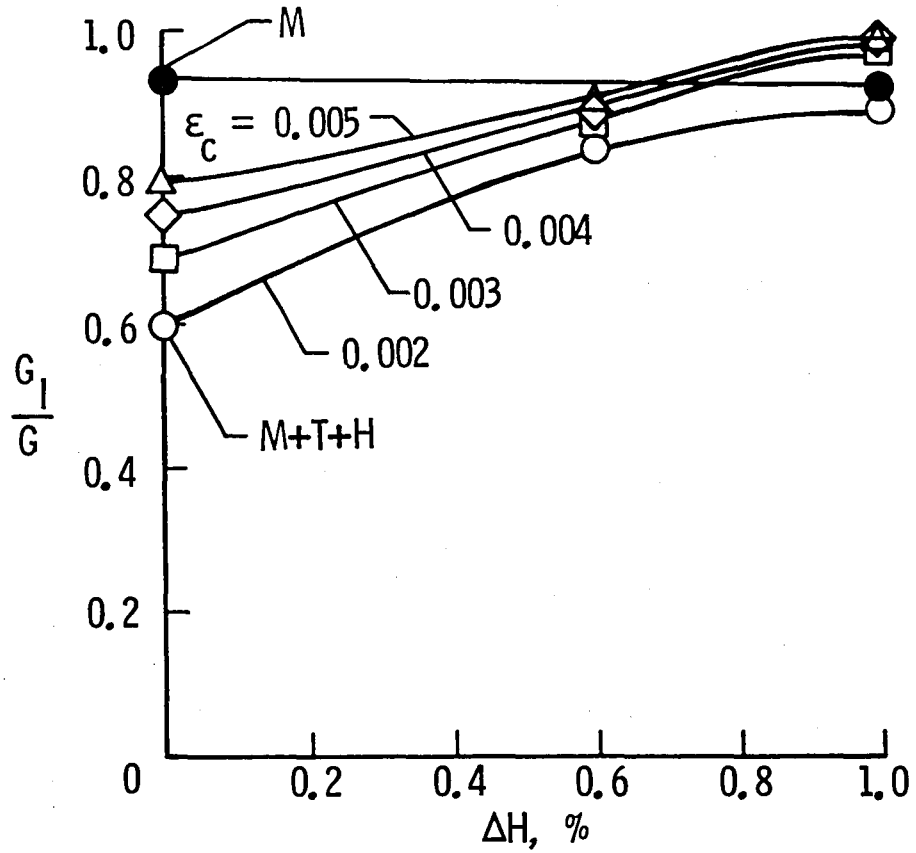

Fig. 9 Effect of Residual Thermal and Moisture Stresses on G_I/G as a Function of Moisture Content and Mechanical Strain

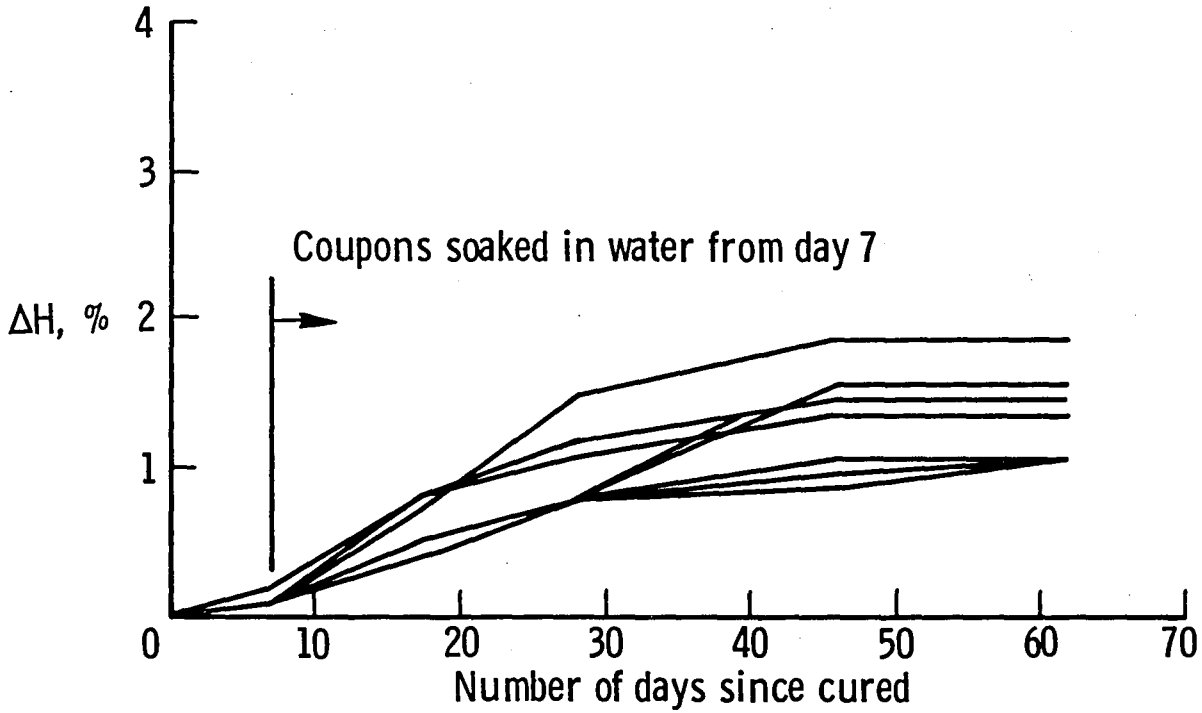

Fig. 10 Measured moisture weight gain with time for T300/5208 $[\pm 35/0/90]_s$ laminates soaked in water.

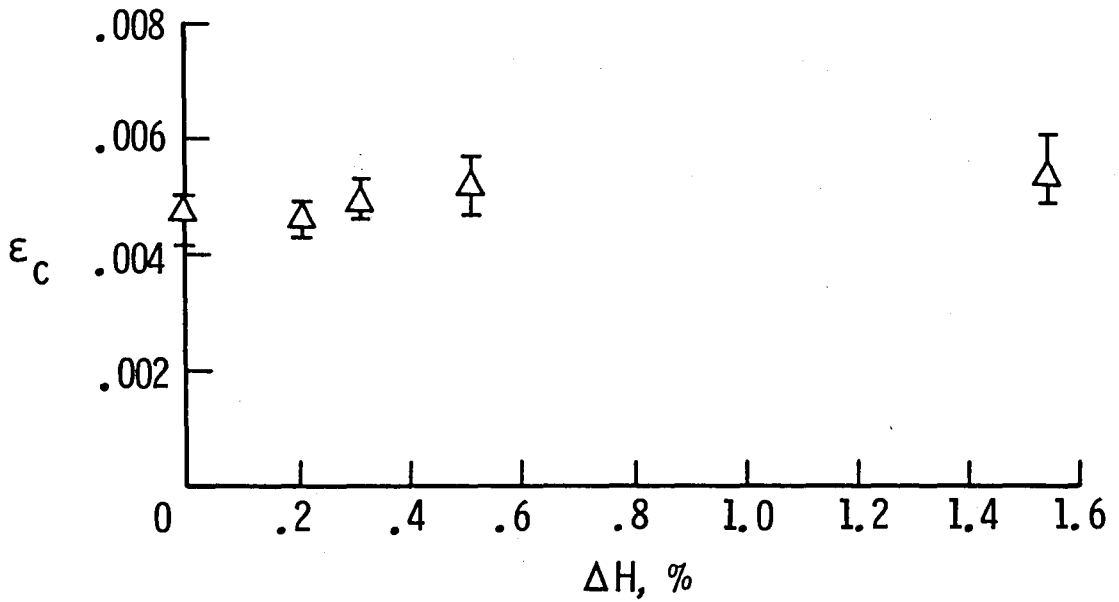

Fig. 11 Influence of moisture on delamination onset strains in $[\pm 35/0/90]_S$ laminates.

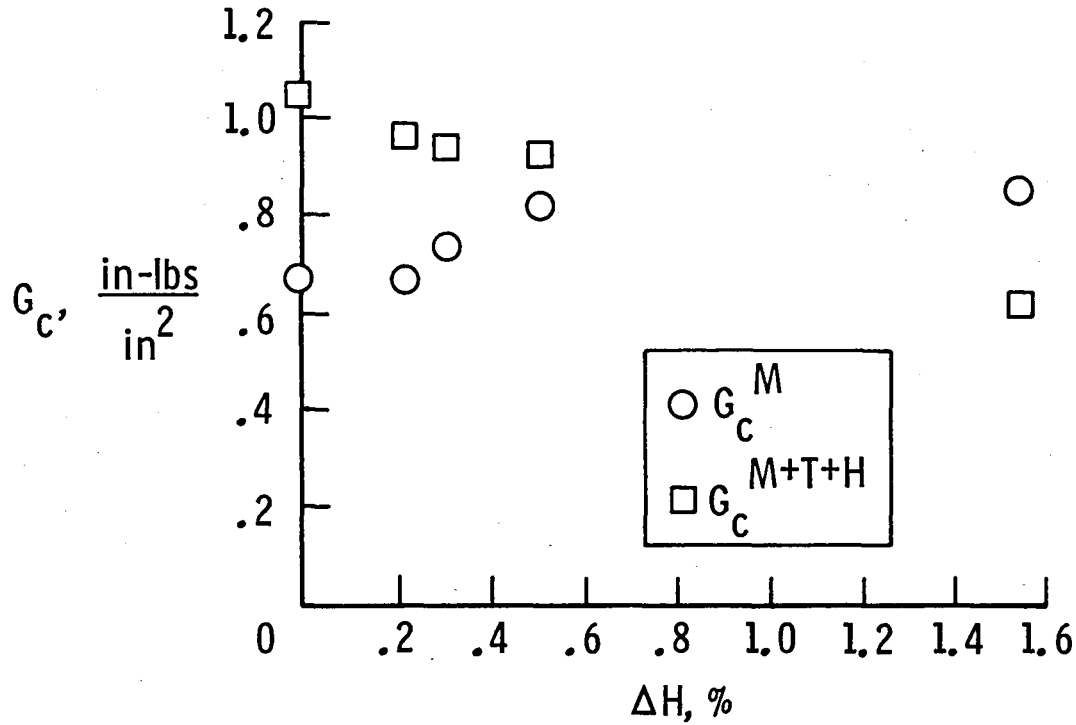

Fig. 12 Influence of moisture and residual thermal stresses on G_c measurement.

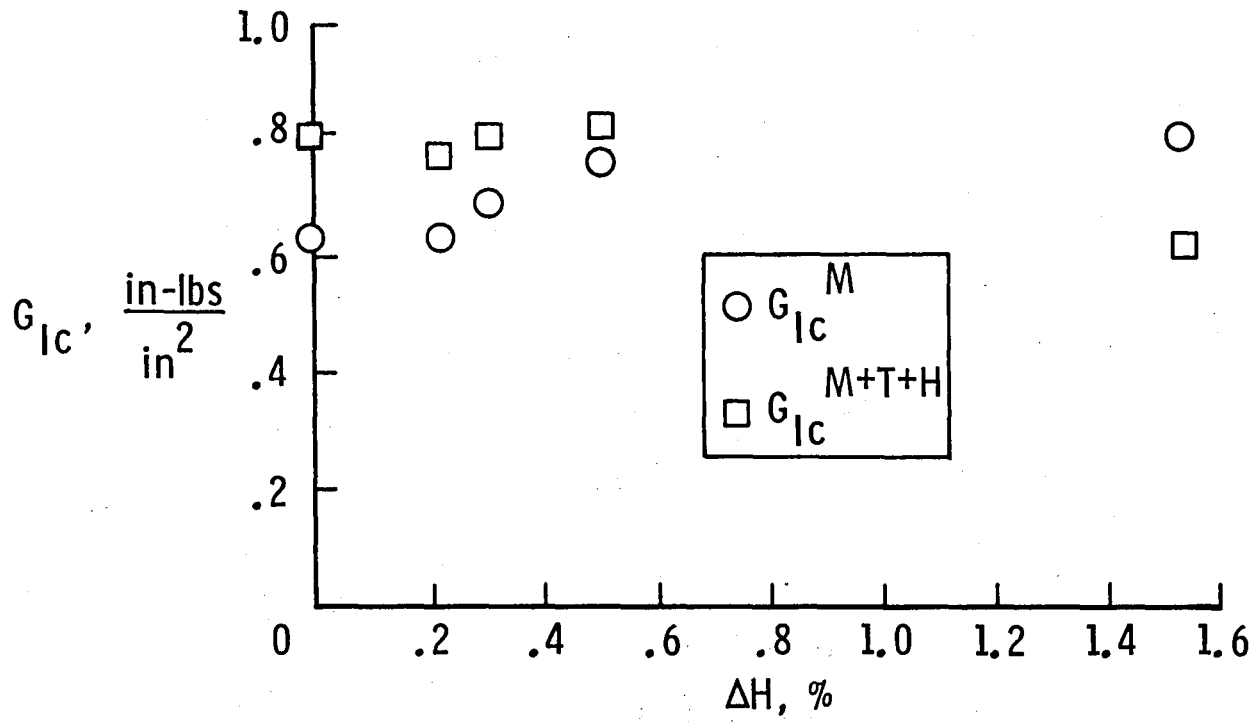

Fig. 13 Influence of residual thermal and moisture stresses on G_{Ic} measurement.

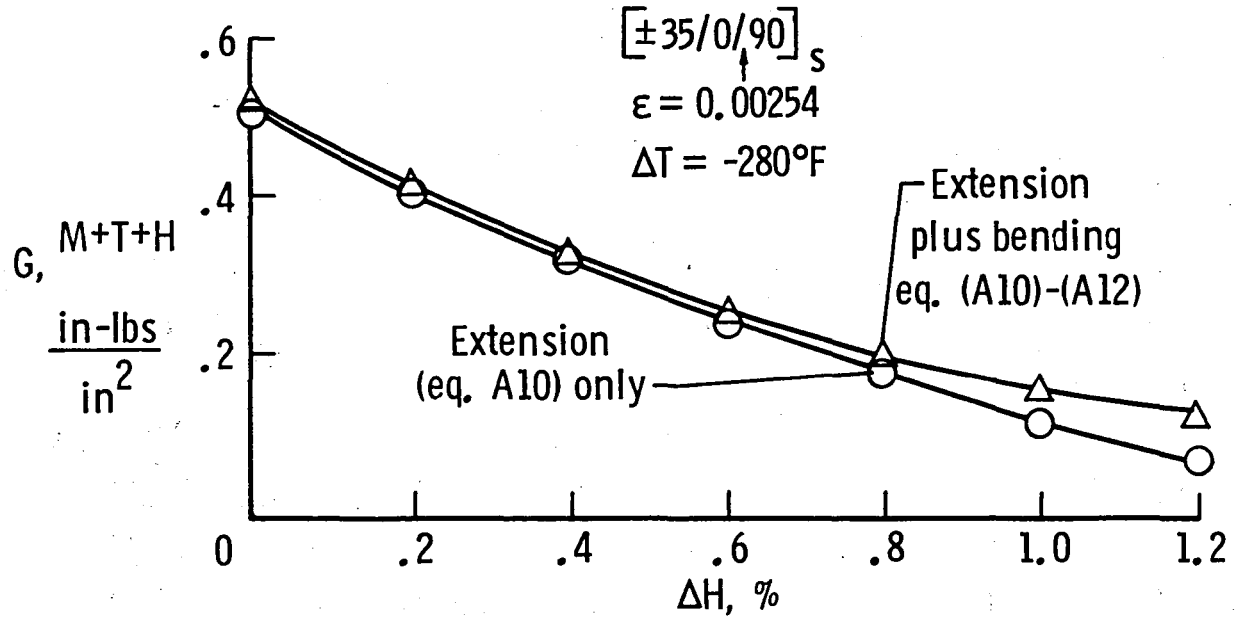

Fig. 14 Strain energy release rate calculation with and without bending/extension coupling.

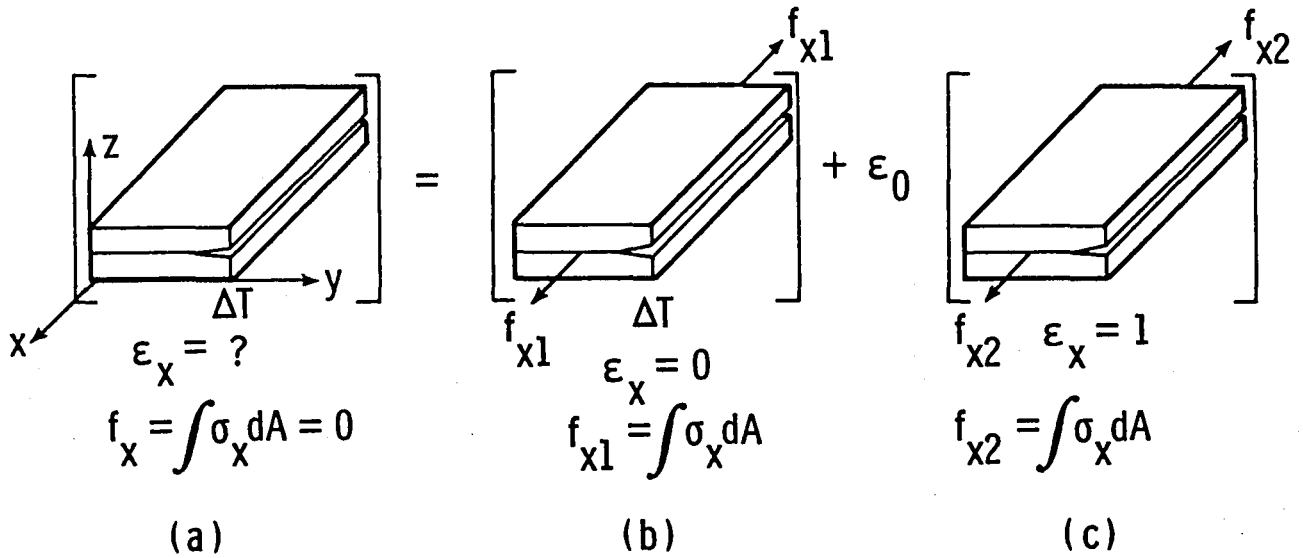

Fig. 15 Thermal stress analysis for delamination using the finite element technique.

1. Report No.	2. Government Accession No.	3. Recipient's Catalog No.
NASA TM-86437 USAAVSCOM TM 85-B-4		

4. Title and Subtitle	5. Report Date
"Residual Thermal and Moisture Influences on the Strain Energy Release Rate Analysis of Edge Delamination"	June 1985
	6. Performing Organization Code: 505-33-33-05
7. Author(s): T. K. O'Brien, I. S. Raju, D. P. Garber	8. Performing Organization Report No.
	10. Work Unit No.
9. Performing Organization Name and Address: NASA Langley Research Center, Hampton, VA 23665; Structures Laboratory, USAAVSCOM Research & Technology Laboratories, Hampton, VA 23665	11. Contract or Grant No.
12. Sponsoring Agency Name and Address: National Aeronautics and Space Administration, Washington, DC 20546 and U.S. Army Aviation Systems Command, St. Louis, MO 63166	13. Type of Report and Period Covered: Technical Memorandum
	14. Army Project No.: 1L161102AH45

15. Supplementary Notes

16. Abstract

A laminated plate theory analysis is developed to calculate the strain energy release rate associated with edge delamination growth in a composite laminate. The analysis includes the contribution of residual thermal and moisture stresses to the strain energy released. The strain energy release rate, G, increased when residual thermal effects were combined with applied mechanical strains, but then decreased when increasing moisture content was included. A quasi-three-dimensional finite element analysis indicated identical trends and demonstrated these same trends for the individual strain energy release rate components, G_I and G_{II}, associated with interlaminar tension and shear. An experimental study indicated that for T300/5208 graphite-epoxy composites, the inclusion of residual thermal and moisture stresses did not significantly alter the calculation of interlaminar fracture toughness from strain energy release rate analysis of edge delamination data taken at room temperature, ambient conditions.

17. Key Words (Suggested by Author(s)): strain energy release rate, residual thermal stress, moisture, delamination, graphite epoxy, composites, fracture mechanics

18. Distribution Statement: Unclassified - Unlimited; Subject Category 24

19. Security Classif. (of this report)	20. Security Classif. (of this page)	21. No. of Pages	22. Price*
Unclassified	Unclassified	49	A03

*For sale by the National Technical Information Service, Springfield, Virginia 22161

End of Document